# An Experimental Study on Thermal Performance of Thermosiphons under Vibration Conditions

**Gokul Depuk T P[1], Annapurna Sogunuru[2], Sunil Chandel[3], Suresh Srivastava[4]**

**Abstract**

Use of thermosiphon for airborne applications depends upon heat transfer ability under vibration conditions. To verify thermal performance of themosiphons, experimental investigations are carried out by attaching them to an X-band Transmit Receive Multi Module(XTRMM). Surface temperatures are measured. Comparative analysis is made with and without attachment of thermosiphons. Thermal performance is measured for thermosiphon at various inclinations. Two phase thermosiphons, copper filled with acetone with a fill ratio of 35-40% are used for experimentation. Experimental set up is subjected to random vibrations ranging from 20-2000Hz. Thermal and functional performance of XTRMM is checked for the same inclinations.

[1] CABS, DRDO, Bangalore-560037 & DIAT, DRDO, Pune- 411025
[2]CABS, DRDO, Bangalore-560037
[3]DIAT, DRDO, Pune- 411025
[4]CABS, DRDO, Bangalore-560037

**Keywords:** Thermosiphon, XTRMM, Thermal performance

## I. Introduction

Thermosiphon is a passive, cost effective and efficient heat transfer device [1]. It is a vessel that is charged with a working fluid after evacuating the air inside it and is sealed at both the ends. It has usually three sections, evaporator, adiabatic and condenser sections. The working fluid is circulated without the aid of any pumps. In two phase thermosiphons, when heat is applied at evaporator section, the latent heat of evaporation, leads pool boiling of the fluid. The vaporised fluid travels to condenser portion through adiabatic portion due to buoyancy forces. When the condenser section is maintained at a temperature at or lower temperatures than the saturation temperature of the vapour, the vapour condensates on the walls. Due to increase in density, the condensed fluid falls back to evaporator section and cycle gets completed. Some thermosiphons may not have adiabatic sections. Figure.1 show the schematic of a thermosiphon and a heat pipe.

Heat pipes are a little complex in construction compared to thermosiphons due to wick structure as shown in Figure.1, but they can operate in any orientation. Thermosiphons are widely utilized in different applications like the solar water heater [1], renewable energy [2-4], air conditioners [5], removing heat from the electronic devices [6-8] and heat recovery [9], machining operations [10] because of the

advantages such as simplicity, excellent performance, and low cost.When it comes to airborne applications, thermosiphons need to be proven thermally effective under the vibration conditions. This aspect is tested by integrating the thermosiphon with an XTRMM.

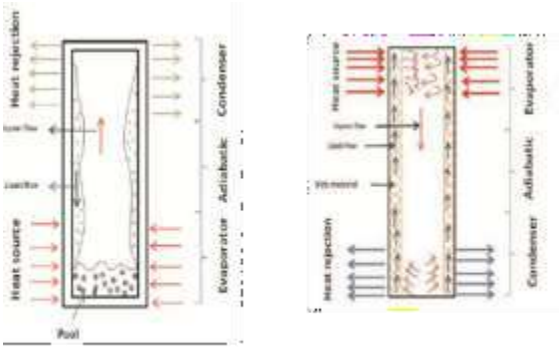


**Figure.1** schematic of thermosiphon and heat pipe

## II. DETAILS OF XTRMM:

XTRMM is a front end electronics unit for X-Band radar. It consists of four channels and generates the Radio Frequency (RF) signals in each channel. These signals are electronically steered and amplified by High Power Amplifiers (HPAs) in transmitter and Low Noise Amplifiers (LNAs) in receivers. These are sensitive and vulnerable to the changing thermal environment during the flight. Due to the high heat flux density of these semiconductor devices, for consistent, safe and reliable operation them proper thermal management is essential. Due to the compactness of the liquid cooling system, XTRMM is preferred to be liquid cooled.

## III. DETAILS OF THERMOSIPHON

Thermosiphons used for the current study are made up of copper tube with 6.1mm diameter and 0.5mm wall thickness. Acetone is used as coolant. Six thermosiphons are used for the experiment. Among the six, five are of length 200mm and one is of 220mm. Filling ratio of the five is 50% and for the sixth one it is approximately 35%.

Flooding limit of the thermosiphon is calculated using the formula:

$$Q_{max,flood} = \frac{T\ h\ \pi D^2\ [g\sigma(\rho\ -\rho\ )^{1/4}]}{[\rho_v^{-0.25} + \rho_l^{-0.25}]^2}$$

$$T_b = \left(\frac{\rho_l}{\rho_v}\right)^{0.14} \tanh^2(B_0)^{1/4}$$

$$B_0 = D_{pipe,in}\left[\frac{g(\rho\ -\rho\ )^{1/2}}{\sigma}\right]$$

And critical heat flux is calculated by the formula

$$Q''_{CHF} = 0.149\rho_v\ -\rho_{lv}\ \left[\frac{\sigma g(\rho\ -\rho\ )^{1/4}}{\rho_v^{2}}\right]$$

$$L_{evap} \geq \pi D \frac{Q}{{}_{pipe}Q''_{CHF}}$$

where Nusselt number is defined as

h L

$$\frac{Nu}{K_l} = \frac{{}_c \; {}_c}{} = \left[\frac{\rho_l^1(\rho_l - \rho_v)gh_{lv}L_c^3}{4\mu_l K_l(T_{sat} - T_{c,i})}\right]^{/4}$$

$$Q = h_c(2\pi R_{pipe,i}L_c)(T_{sat} - T_{c,i})$$

## IV. EXPERIMENTATION

Experiments on XTRMM are conducted in incremental phases.

## Iv. I phase-I Experiments And Results

These experiments were carried out initially to assess the effectiveness of the thermosiphons in cooling XTRMM. These are:

(i) XTRMM alone with just power ON, (ii) XTRMM alone with RF ON

(iii) XTRMM with RF ON, integrated with Aluminium(Al) block

(iv) XTRMM with RF ON integrated with Aluminium block embedded with thermosiphons

(v) XTRMM with RF ON integrated with Aluminium block embedded with thermosiphons exposed to air flow at 3.5m/s induced by fan

All the above experiments are carried out at 25.60Cambient temperature. During these experiments, XTRMM is positioned on a thermocol sheet. Temperature on the surfaces of XTRMM and thermosiphons is measured using a calibrated k-type thermocouple. Accuracy of the thermocouples is 0.080C.These thermocouplesare connected to a data logger for monitoring the temperature at an interval of one second. Aluminium block of used to attach XTRMM is of dimensions 113mm x115mmx17mm has 6.25mm diameter holes pre drilled, up to a depth of 30mm one of the face having dimensions113mmx17mm. for the test cases(iv) and (v), inclination of thermosiphons is kept in between 200-300 with horizontal surface table.

It is specified by manufacturer that surface temperature of XTRMM should not exceed 600C.Hence experiments are stopped when thesurface temperature is reached either to600C or to steady state condition. When the temperature values are fluctuating within ±0.50C from the mean value, for continuously 10-15 minutes is treated as steady state condition for the present experiments.Table-I shows the test cases, test duration and the surface temperature measured for each test case.

**Table-I:** Experimental results

| Test case | Power, W | Test Case | Surface temperature XTRMM | Test duration, sec |
|---|---|---|---|---|
| 1 | 9.5 | XTRMM power ON | 59.4 | 480 |
| 2 | 17.2 | XTRMM RF ON | 60.9 | 390 |
| 3 | 17.2 | XTRMM integrated with Al block RF ON | 58.9 | 5310 |
| 4 | 17.2 | XTRMM integrated with Al block embedded with thermosiphons RF ON | 50.5 | 3990 |
| 5 | 17.2 | XTRMMwith Al block embedded with fan(3.2m/s) cooled thermosiphons RF ON | 35.5 | 1680 |

**Figure.2** Test set up for Phase-I Experiments

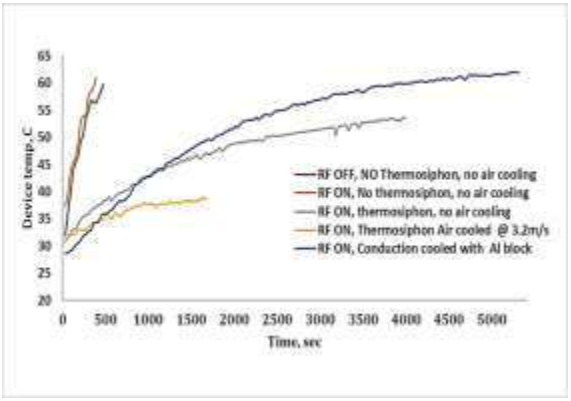


**Figure.3** Time vs XTRMM Surface temperature for test cases

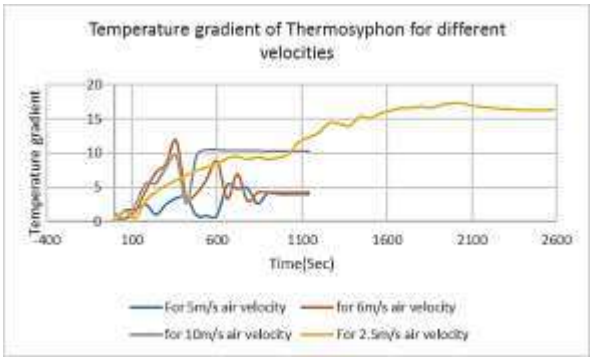


**Figure.4** Temperature gradient of thermosiphon for different velocities

## Iv. Ii Phase-Ii Experiments: With Vibration Test Fixture And Results

**Phase-II experiments are conducted for XTRMM attached Al block embedded with thermosiphons along with the vibration fixture.**

The vibration fixture is made to facilitate XTRMM test setup to the vibration table. The fixture details are shown in a schematic block diagram in Figure 4. The fixture base plate is drilled with holes of the same size and pitch to that of the vibration table. These holes enable firm fixing using bolts, during the vibration tests. The Al block is positioned inbetween two L-members using two L-angles underneath. The L-members on both sides have holes at 300, 600, and 900 at one end and a single hole on the other end. This arrangement enables Al block rotation to any of test the angles said above. On one face of 113mmx115mm size, XTRMM is attached. On the other face, a back plate is attached. Thermosiphons are clamped to this back plate in order to prevent any movement.

Similarly, one Al strip is provided to clamp the thermocouples to Al block to prevent movement of them(Figure.4). All the attachments are made using appropriate bolts along with suitable washers.

Due to the increase in thermal conduction path by the additional attachment of vibration fixture, experiments are repeated to verify thermal performance of XTRMM and thermosiphons. These tests are conducted for all the three angles.

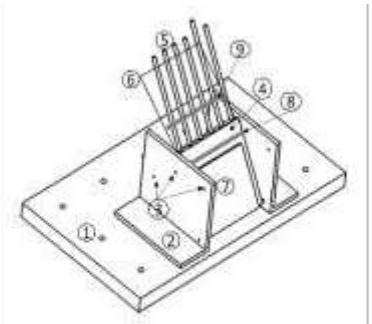


**Figure 5.** Schematic of vibration test fixture

**Figure 6.** Test setup with Vibration Fixture for Phase-II experiments

**Table-II:** Experimental results with vibration fixture

| Test case | Power, W | Thermosiphon inclination | Surface temperature XTRMM | Test duration, sec |
|---|---|---|---|---|
| 1 | 15.7 | 30 | 30.5 | 2000 |
| 2 | 15.7 | 60 | 31 | 2000 |
| 3 | 15.7 | 90 | 29.5 | 2000 |

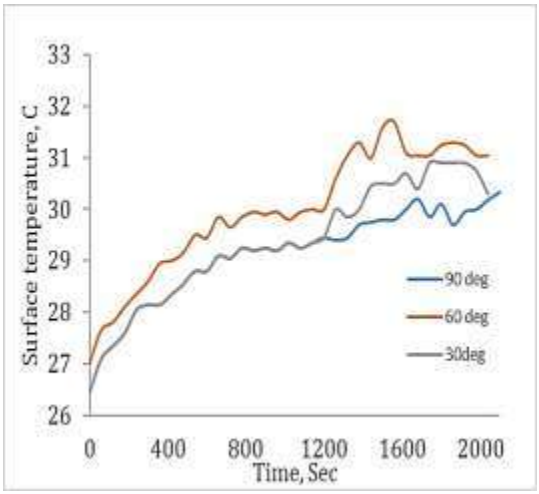


**Figure.7** Time vs XTRMM Surface temperature for different thermosiphon angles

## Iv.iii. Phase-iii experiments: vibration tests and results

In order to verify the thermal performance of thermosiphons under vibration conditions, it is planned to conduct Random Vibration test within band width 20-2000Hz. From previous measured data for of external mounted equipment on the aircraft is measured as 4.66 GRMS []. Hence to sweep across a band of 20Hz -2000Hz for random vibration tests, Acceleration Spectral Density(ASD) is calculated as 0.01g2/Hz. The test setup mounted on the vibration table is shown in Figure 7.

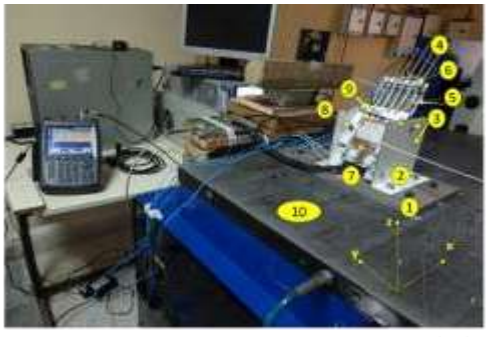


**Figure 8.** Vibration test setup

Initially the test setup is subjected to resonance search between a sweep of 20Hz to 2000Hz. When the vibration monitor sensor is attached to L-Member, it is observed that vibration levels are amplified due to overhang portion. This overhang is the portion of the extra unattached length when the Al block is fixed at one particular inclination out of 300 or 600 or 900. Resonance of fixture is observed between 100Hz to 300Hz as shown in Figure 8.
Since the vibrations are amplified on the compared to table settings, table vibration levels are set at 0.001g2/Hz ASD so that it is enhanced at the XTRMM level. The entire setup is firmly fastened to vibration table and thermocouples are held to the back plate using clamp connections. To prevent movement of thermocouples and other power, RF connecting wires, they are tightly clamped below aluminium strip. At thefree end of thermosiphon, thermocouples are held tightly using tie wraps. Vibration tests are conducted for all 300, 600 and 900 angles for x, y and z directions. The setup directions are as denoted in the Figure.7.

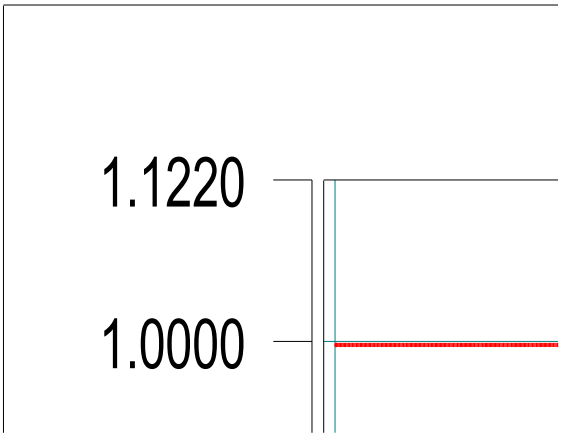


**Figure 9.** Initial Resonance search for test fixture

PSD spectrums plotted for the test angles of thermosiphon 300, 600 and 900 along x-axis are shown in Figure 9, Figure 10 and Figure 11. Temperature measured on the XTRMM surface during these tests are shown in Figures 12. All vibrations tests are conducted until the temperature temperature measured on the surfaces have reached to a steady state at least for 15min to 20minutes.

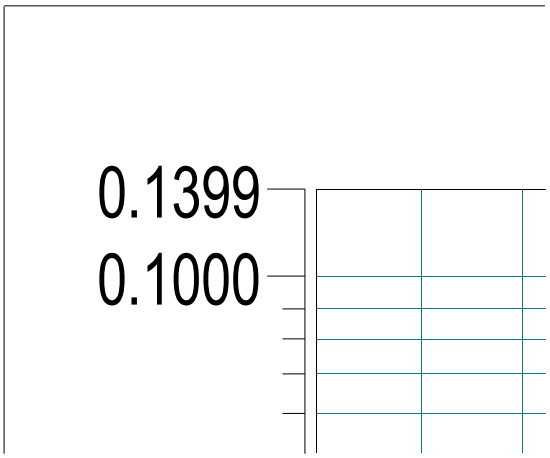


**Figure 9**. PSD spectrum for x-axis, 300 inclination of thermosiphon

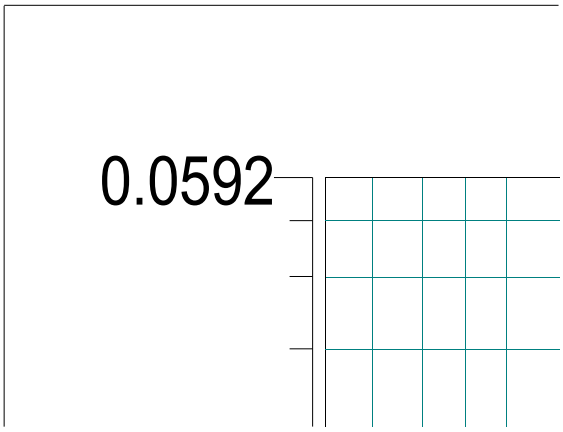


**Figure 10.** PSD spectrum for x-axis, 600 inclination of thermosiphon


**Figure 11.** PSD spectrum for x-axis, 900 inclination of thermosiphon

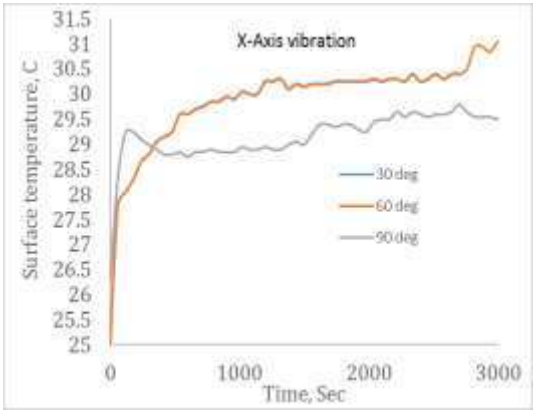


**Figure 12**. Surface temperature of XTRMM during vibration test along x-axis

PSD spectrums plotted for the test angles of thermosiphon 300, 600 and 900 along y-axis are shown in Figure 13, Figure 14 and Figure 15. Temperature measured on the XTRMM surface during these tests are shown in Figures 16.

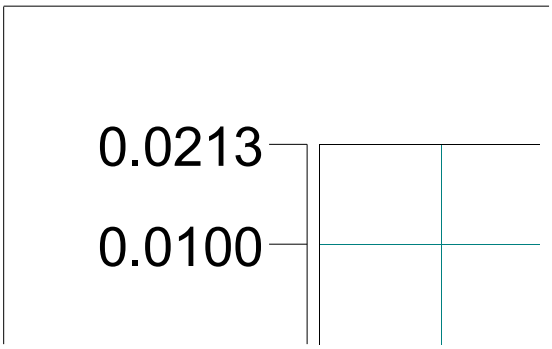


**Figure 13**. PSD spectrum for y-axis, 300 inclination of thermosiphon

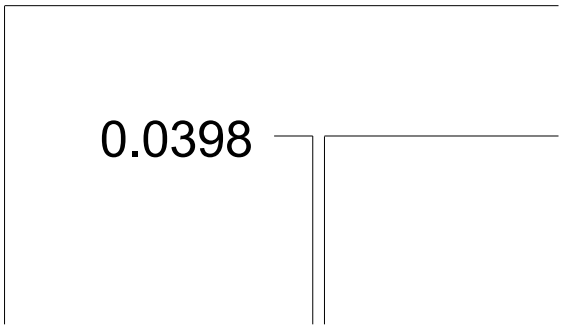


**Figure 14**. PSD spectrum for y-axis, 600 inclination of thermosiphon

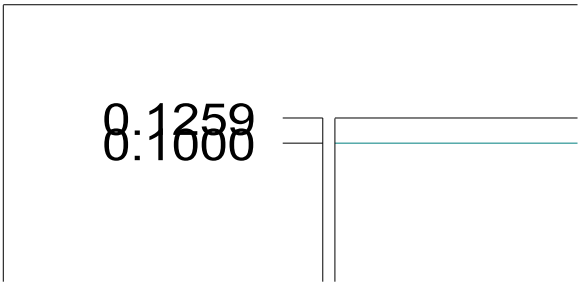


**Figure 15**. PSD spectrum for y-axis, 900 inclination of thermosiphon

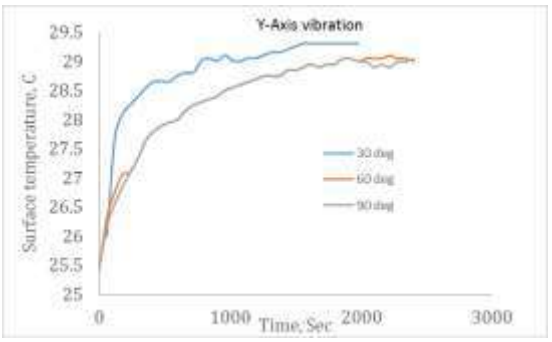


**Figure 16.** Surface temperature of XTRMM during vibration test along y-axis

PSD spectrums plotted for the test angles of thermosiphon 300, 600 and 900 along z-axis are shown in Figure 17, Figure 18 and Figure 19. Temperature measured on the XTRMM surface during these tests are shown in Figures 20.

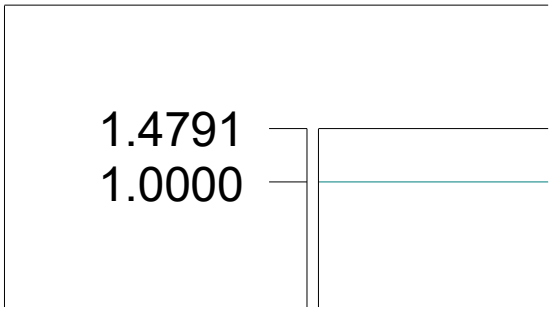


**Figure 17**. PSD spectrum for z-axis, 300 inclination of thermosiphon

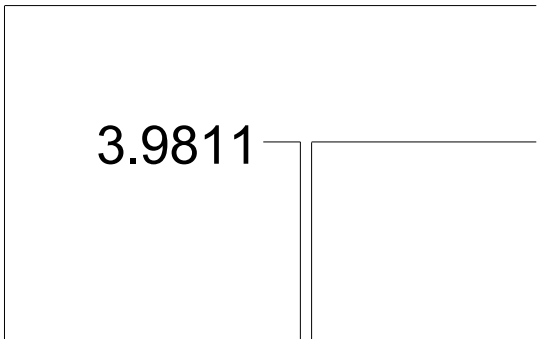


**Figure 18.** PSD spectrum for z-axis, 600 inclination of thermosiphon

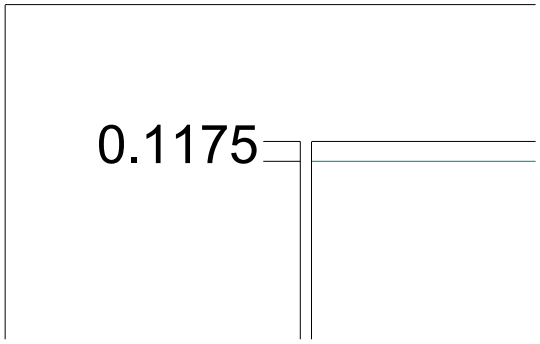


**Figure 19.** PSD spectrum for z-axis, 900 inclination of thermosiphon

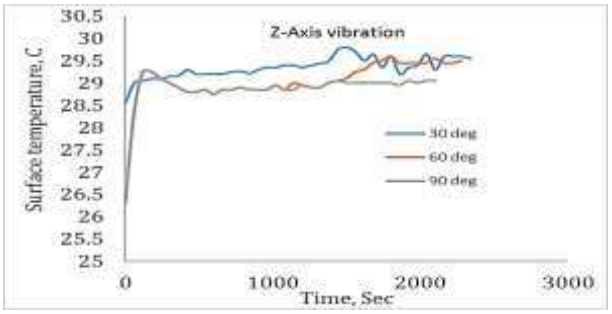


**Figure 20**. Surface temperature of XTRMM during vibration test along z-axis

## V. Conclusions

Experimental studies are conducted to verify thermal performance of thermosiphon integrating with XTRMM. Cooling is significantly improved with attachment of thermosiphon. Tests are conducted for different air flow velocities. As the air flow rate is increased on the condenser portion of thermosiphon, XTRMM surface temperature has reached to steady state temperature quickly. Maximum surface temperature measured on the XTRMM is less by 10C- 20C to that of the surface temperature measured during vibration tests. For the z-axis vibration tests, steady state is attained quickly compared to x-axis and y-axis vibration tests. Short length of the thermosiphons and vertical oscillations could have resulted in better heat transfer. These inputs may be used for thermal management of avionic equipment.

## Acknowledgements

Authors acknowledge Director, CABS for permitting to utilise vibration test facility. They acknowledge the support extended by CABS QAG team, Mr. Anand, Ms. Savitha, Ms. Dheepthi and Mr. Abhishek during experimentation.

## References

1. Wei Zhong, Wenhui Ji, 'Applications of coupling thermosiphons with phase change materials': A review, Energy & Buildings 233 (2021) 110690. Doi:10.1016/j.enbuild.2020.110690
2. Messaoud Badache, Zine Aidoun, Parham Eslami-Nejad, Daniela Blessent, 'Ground-Coupled Natural Circulating Devices (Thermosiphons): A Review of Modeling,Experimental and Development Studies,Inventions 2019, 4, 14 doi:10.3390/inventions4010014
3. M.G. Hammouda a, D. Ewing a, A. Zaghlol b, C.Y. Ching, ' Heat Transfer Performance in a Vertical Grooved Thermosiphon', International Journal of Thermofluids, 11 (2021) 100107, https://doi.org/10.1016/j.ijft.2021.100107
4. Rong-Horng Chen, LW Kuo,Chi-Ming Lai 'The influence of longitudinal vibrations on the heat transfer performance of inclined heat pipes', Advances in Mechanical Engineering, DOI: 10.1177/1687814015568940
5. Sarah H. Ali, Adel A. Eidan, Assaad Al Sahlani, M.J. Alshukri, Ahmad Q. Ahmad 'The Effect of Vibration Pulses on the Thermal Performance of Evacuated Tube Heat Pipe Solar Collector', Journal of Mechanical Engineering Research and Developments, Vol. 43, No. 4, pp. 340-347, 2020
6. H.Jouhara, A.Chauhan, T.Nannau, S.Almahmoud, B.Delpech, I.C.Wrobel 'Heat pipe based systems - Advances and applications', Energy 128(2017) 729-754, doi: 10.1016/j.energy.2017.04.028
7. Claudio Zilioa, Giulia Righettia, Simone Mancina, Romain Hodotb, Claude Sarnob,Vincent Pommec, Bertrand Truffart 'Active and passive cooling technologies for thermal management of avionicsin helicopters: Loop heat pipes and Mini-Vapor Cycle System' Thermal Science and Engineering Progress 5 (2018) 107–116, doi:10.1016/j. tsep.2017.11.002
8. 'Heat transfer calculations of a thermosiphons' October 2014, Qpedia
9. Nkosana Ignetious Ncaba, Nyuytifo Emmanuel Wiykiynyuy, Tien-Chien Jen, Kingsley Ukoba, 'Effect of Thermosyphon Limits on Design of A Taper Thermosyphon Drill for Dry Drilling Operation' , 2020 IEEE 11th International Conference on Mechanical and Intellligent Manufacturing Technologies
10. Ahmed A. Alammar, Raya K.Al-Dadah, Saad M.Mahmoud 'Experimental investigation of theinfluence of the geyser boiling phenomenon on the thermal performance of a two-phase closed thermosyphon', Journal of cleaner Production xxx(2017)1-13, doi:10.1016/j.jclepro.2017.11.157
11. K.Prisniakova,O.Marchenko,Yu.Melikaev,V.Kravetz,Yu.Nikolaenko,V.Prisniakov 'About the complex influence of vibrations and gravitational fields on serviceability of heat pipes in composition of space-rocket system' , Acta Astronautica 55 (2004) 509–518, doi:10.1016/j.actaastro.2004.05.005
12. Marcia Barbosa Henriques Mantelli, Thermosyphons and Heat Pipes: Theory and Applications, Springer(eBook), doi: 10.1007/978-3-030-62773-7
13. Christina A. Pappas, Paul M. De Cecchis, Donald A. Jordan, Pamela M. Norris ' The Effect of Fill Volume on Heat Transfer From Air-Cooled Thermosyphons', Journal of Heat TransferApril 2013, Vol.135/044504-1
14. Yafeng Wu, Zhe Zhang, Wenbin Li, Daochun Xu, 'Effect of the Inclination Angle on the Steady-State Heat Transfer Performance of a Thermosyphon', Applied Sciences, 2019, 9, 3324, doi:10.3390/app9163324
15. B.Jiao, L.M.Qiu, X.B. Zhang, Y.Zhang 'Investigation on the effect of filling ratio on the steady-state heat transfer performance of a vertical two-phase closed thermosyphon' Applied Thermal Engineering 28(2008) 1417-1426, doi: 10.1016/j.applthermaleng.2007.09.009
16. M. Alizadeha, D. D. Ganjia, 'Heat transfer characteristics and optimization of the efficiency and thermal resistance of a finned thermosyphon', Applied Thermal Engineering,doi.10.1016/j.applthermaleng. 2020.116136